Epigenetic downregulation of the proapoptotic gene *HOXA5* in oral squamous cell carcinoma

YING-JU CHEN[1*], SHIN-WEI LIAO[1*], YEN-LING LAI[1], YU-FEN LI[2], YIN-CHE LU[3,4] and CHIEN-KUO TAI[1]

[1]Department of Biomedical Sciences, National Chung Cheng University, Chia-Yi 62102, Taiwan, R.O.C.;
[2]Department of Public Health, China Medical University, Taichung 40402, Taiwan, R.O.C.;
[3]Division of Hematology-Oncology, Ditmanson Medical Foundation Chia-Yi Christian Hospital, Chia-Yi 60002, Taiwan, R.O.C.;
[4]Min-Hwei Junior College of Health Care Management, Tainan 73658, Taiwan, R.O.C.

Received July 16, 2024; Accepted November 26, 2024

DOI: 10.3892/mmr.2024.13421

Abstract. Homeobox A5 (*HOXA5*) has been identified as a tumor suppressor gene in breast cancers, but its role in oral squamous cell carcinoma (OSCC) has not been confirmed. The Illumina GoldenGate Assay for methylation identified that DNA methylation patterns differ between tumorous and normal tissues in the oral cavity and that *HOXA5* is one of the genes that are hypermethylated in oral tumor tissues. The present study obtained more-complete information on the methylation status of *HOXA5* by using the Illumina Infinium MethylationEPIC BeadChip and bisulfite sequencing assays. The results indicated that *HOXA5* hypermethylation has great potential as a biomarker for detecting OSCC. Comparing *HOXA5* RNA expression between normal oral tissue and OSCC tissue samples indicated that its median level was 2.06-fold higher in normal tissues that in OSCC tissues. Moreover, treatment using the demethylating agent 5-aza-2'-deoxycytidine can upregulate *HOXA5* expression in OSCC cell lines, verifying that the silencing of *HOXA5* is primarily regulated by its hypermethylation. It was also found that upregulation of *HOXA5* expression can not only increase OSCC cell death but that it can also enhance the therapeutic effect of cisplatin both *in vitro* and *in vivo*, suggesting that *HOXA5* is an epigenetically downregulated proapoptotic gene in OSCC.

Correspondence to: Professor Chien-Kuo Tai, Department of Biomedical Sciences, National Chung Cheng University, 168 University Road, Min-Hsiung, Chia-Yi 62102, Taiwan, R.O.C.
E-mail: biockt@ccu.edu.tw

Dr Yin-Che Lu, Division of Hematology-Oncology, Ditmanson Medical Foundation Chia-Yi Christian Hospital, 539 Zhongxiao Road, Chia-Yi 60002, Taiwan, R.O.C.
E-mail: 04688@cych.org.tw

*Contributed equally

Key words: oral squamous cell carcinoma, DNA methylation array, homeobox A5, p53, apoptosis

Introduction

Oral cancer is one of the most common cancers worldwide (1,2). The 2021 cancer registry annual report from the Ministry of Health and Welfare of Taiwan revealed that the age-adjusted incidence and mortality rates of oral cancer in males were 40.38/100,000 and 16.38/100,000, respectively, making it the fourth most common cause of cancer-related mortality among males in Taiwan (3). Other than cigarette smoking and alcohol drinking, betel nut chewing is the main risk factor for oral cancer and ~90% of patients in Taiwan are habitual betel nut chewers (4). Oral squamous cell carcinoma (OSCC) is the main subset or oral cancer, accounting for >90% of cases and has a poor prognosis (5). The standard treatments for OSCC include surgery, chemotherapy and radiotherapy (6). However, the 5-year survival rate of OSCC is ~50% due to the poor responses to chemotherapy and radiotherapy resulting in recurrence and worse outcomes (7,8). However, the survival rate could be improved to ~80% if patients identify the symptoms and seek medical advice early, allowing them to be diagnosed in the initial stage and undergo the standard treatments (9,10). It is therefore important to identify reliable biomarkers for detecting OSCC.

Epigenetic alterations, particularly hypermethylation in the promoter region of tumor suppressor genes, have been identified as biomarkers for a number of cancers including OSCC and play a critical role in oral cancer development (11). A number of genes responsible for cell-cycle events, apoptosis, cell-to-cell adhesion and DNA repair are found to be hypermethylated and silenced in OSCC (12). We have previously used the Illumina GoldenGate Assay to identify the DNA methylation status of 1,505 CpG sites encompassing 807 genes in 40 OSCC tissue and 15 normal samples. The methylation array data was used to identify the gene Homeobox A5 (*HOXA5*), which is hypermethylated in OSCC samples (13).

HOXA5 is a member of the *Hox* gene family that plays an important role in embryonic development due to its transcriptional activation ability (14,15). A previous study found that HOXA5 protein is a positive regulator of p53 transcription and function in breast cancer cells, indicating that reduced *HOXA5* expression is an important step in tumorigenesis (16). Moreover, the effects of *HOXA5* in various cancers have gradually been

elucidated over the past two decades. *HOXA5* is downregulated by epigenetic alterations in breast cancer (17,18), lung adenocarcinoma (19) and xanthoastrocytoma (20), but upregulated in hepatocellular carcinoma (21). Aberrant expression of *HOXA5* was also observed in OSCC; however, the epigenetic regulation and role of *HOXA5* in OSCC has not been fully investigated (22).

The present study first examined the methylation status of *HOXA5* in OSCC tissues by using techniques such as the bisulfite sequencing assay and Illumina Infinium MethylationEPIC BeadChip analysis (Illumina, Inc.). The expression level of *HOXA5* was also analyzed to determine whether it differs between normal oral and OSCC tissues in patients with OSCC. The gene expression of *HOXA5* in OSCC cell lines was then restored by using epigenetic drugs and employing lentivirus vector-mediated gene transfer of *HOXA5*. Restoration of *HOXA5* significantly upregulated HOXA5 and p53 expression and induced OSCC cell death. The results strongly suggested that *HOXA5* was a proapoptotic gene that is epigenetically downregulated in OSCC.

Materials and methods

Specimen collection and bisulfite conversion of genomic DNA. The 25 paired OSCC and adjacent normal tissues used in the present study were collected from the tissue bank of China Medical University Hospital in Taiwan. The median age at surgery of the 25 male patients with OSCC from whom tissue was obtained for analysis was 52.0 years (range: 36-63 years). Tissue samples were collected from patients after obtaining written informed consent in accordance with a protocol approved by the Institutional Review Board of China Medical University Hospital (IRB no. CMUH102-REC1-054). Genomic DNA of these tissues and cultured cell lines was extracted using Gentra Puregene Tissue Kit (Qiagen GmbH) and bisulfite conversion of genomic DNA was performed using EZ DNA methylation kit (Zymo Research Corp.). Bisulfite conversed Universal Methylated Genomic DNA (MilliporeSigma) was used as *in vitro* methylated DNA (IVD) control for the methylation analysis.

Reverse transcription-quantitative (RT-q) PCR. Total RNA was extracted from cell lines (70-80% confluence) or tissue specimens using REzol C & T reagent (Protech Technology Enterprise Co., Ltd.) according to the manufacturer's protocol. The aliquots of RNA were then used to synthesize complementary DNA (cDNA) using SuperScript III First-Strand Synthesis System (Thermo Fisher Scientific, Inc.) according to the manufacturer's protocol. RT-qPCR was performed using SYBR Green Realtime PCR Master Mix (Toyobo Life Science) and ABI StepOne real-time PCR system (Applied Biosystems; Thermo Fisher Scientific, Inc.) as the following steps: 95˚C for 5 min, followed by 50 cycles of successive incubation at 95˚C for 30 sec, 62˚C for 30 sec and 72˚C for 45 sec. The primers used to amplify HOXA5 and p53 cDNA were: HOXA5 forward, 5'-GCGCAAGCTGCACATAAG-3' and reverse, 5'-CGG TTGAAGTGGAACTCCTT-3'; p53 forward, 5'-CCGCAG TCAGATCCTAGCG-3' and reverse, 5'-AATCATCCA TTGCTTGGGACG-3'. GAPDH was also amplified as an internal control with primers 5'-TTGACGGTGCCATGG AATTT-3' and 5'-GCCATCAATGACCCCTTCATT-3'. All samples were analyzed in triplicate. The expression levels of HOXA5 and p53 were calculated using the $2^{-\Delta\Delta Cq}$ method (23) and normalized to that of GAPDH.

Bisulfite sequencing assay and quantitative methylation-specific PCR. Bisulfite conversed DNA from tissues was amplified by two pairs of *HOXA5* promoter-specific primers which targeted one *HOXA5* promoter region from -1423 to -841 (forward, 5'-AGGAATAAAGGGGGTTTTAATAGAG-3'; and reverse, 5'-TCCAACCTAAAAAATCTTCATCAC-3') and another promoter region from -505 to -31 (forward, 5'-ATTTTT AAAATTTAGAGTTGTTGGTAGGA-3'; and reverse, 5'-CTA AAACATATACTTAATTCCCTCCTA-3') upstream of the *HOXA5* transcription start site (TSS). As treatment of DNA with sodium bisulfite converts unmethylated C to U, which is subsequently converted to T during PCR amplification, the forward primers for bisulfite sequencing assay are devoid of C, while the reverse primers are devoid of G. The PCR products were separated by gel electrophoresis, purified with a QIAquick gel extraction kit (Qiagen GmbH) and cloned into the yT&A cloning vector (Yeastern Biotech Co., Ltd.) followed by DNA sequencing. For quantitative methylation-specific PCR (MSP), the region from-268 to -59 upstream of the TSS of *HOXA5* was amplified for bisulfite converted DNA from cultured cells with the primers as followed: Forward, 5'-AGTTTTGTTTTT AGCGGGTGGC-3'; and reverse, 5'-GTAAACACCCAAATA TAAAATACGAC-3'. Quantitative MSP was performed using SYBR Green Realtime PCR Master Mix (Toyobo Life Science) and ABI StepOne real-time PCR system (Applied Biosystems; Thermo Fisher Scientific, Inc.) using the following steps: 95˚C for 5 min, followed by 45 cycles of successive incubation at 95˚C for 30 sec, 58˚C for 30 sec and 72˚C for 45 sec. A DNA fragment devoid of any CpG dinucleotide in *COL2A1* was amplified as an input control for quantitative MSP with the primers as followed: forward, 5'-GGGAAGATGGGA TAGAAGGGAATAT-3'; reverse, 5'-TCTAACAATTATAAA CTCCAACCACCAA-3'. For each sample, the threshold cycle number of methylated *HOXA5* and *COL2A1* were determined. The percentage of *HOXA5* methylation was calculated using the $2^{-\Delta\Delta Cq}$ method as the ratio of *HOXA5* to *COL2A1* of a sample divided by the same ratio of IVD.

Cell culture. The OSCC cell lines OC2 and OCSL (obtained from Dr Yong-Kie Wong, Department of Dentistry, Taichung Veterans General Hospital, Taichung, Taiwan) (24,25), established from surgical specimens of buccal mucosa squamous carcinoma from two Taiwanese male patients who had the habits of betel nut chewing, alcohol drinking and cigarette smoking, were maintained in RPMI 1640 medium (Gibco; Thermo Fisher Scientific, Inc.) supplemented with 10% fetal bovine serum (FBS, Invitrogen; Thermo Fisher Scientific, Inc.). They are immortalized cancer cells with unlimited growth potential and have been characterized by tumorigenesis in nude mice. The transformed human embryonic kidney cell line 293T (ATCC; CRL-3216) was grown in DMEM medium (Gibco; Thermo Fisher Scientific, Inc.) supplemented with 10% FBS. *Mycoplasma* negativity was confirmed before all cell experiments.

5-aza-2'-deoxycytidine treatment. Cells were seeded at a density of $1x10^6$ cells in 10-cm culture dishes and treated with 0.5 μM or 5 μM 5-aza-2'-deoxycytidine (5-Aza-dC; (MilliporeSigma). At 72 h post-treatment, cells were harvested and their DNA, RNA and proteins were extracted.

Western blot analysis. Cells were lysed by RIPA Lysis & Extraction Buffer with protease inhibitor cocktail (Thermo Fisher Scientific, Inc.) according to the manufacturer's protocol. A BCA protein assay kit (Thermo Fisher Scientific, Inc.) was used to measure the protein concentration in cell lysates. Proteins (20 μg/lane) in cell lysates were resolved using SDS-10% polyacrylamide gel electrophoresis and transferred onto polyvinylidene difluoride membranes (Bio-Rad Laboratories, Inc.). The membranes were blocked for 2 h at room temperature in TBST with 5% non-fat dry milk (Bio-Rad Laboratories, Inc.) and incubated overnight at 4˚C with antibodies against HOXA5 (1:1,000 dilution; cat. no. sc-81289; Santa Cruz Biotechnology, Inc.), p53 (1:1,000 dilution; cat. no. sc-126; Santa Cruz Biotechnology, Inc.) and GAPDH (1:1,000 dilution; cat. no. sc-47724; Santa Cruz Biotechnology, Inc.). Subsequently, the membranes were incubated with a horseradish peroxidase-conjugated secondary antibody (1:10,000 dilution; cat. no. 31430; Thermo Fisher Scientific, Inc.) for 1 h at room temperature. The specific protein signals were detected using an enhanced chemiluminescence kit (cat. no. WBKLS0500; MilliporeSigma). Quantification of HOXA5 and p53 band intensities was determined using ImageJ software v1.49 (National Institutes of Health) and normalized to that of GAPDH.

Plasmid construction and lentivirus vector production. The full-length human *HOXA5* cDNA was amplified from the immortalized ovarian surface epithelia cell line IOSE (26) by RT-PCR. The amplicon was cloned into a 2nd generation lentiviral vector plasmid pSin-IRES-GFP (IG) (27) at the *Xba*I and *Eco*RI sites to generate pSin-HOXA5-IRES-GFP (HIG). The plasmids pIG or pHIG (12 μg) were cotransfected with lentiviral packaging plasmids pCMVdeltaR8.91 (10.8 μg) and pMD.G (1.2 μg) (obtained from the National RNAi Core Facility, Taipei, Taiwan) into 293T cells. At 48 h post-transfection the lentivirus-containing supernatants were collected and filtered through 0.45-μm pore size filters (MilliporeSigma) prior to use in transduction assays. Lentiviral vector stock at a multiplicity of infection (MOI) of 5 was used to infect OSCC cells. Successful infection of lentiviral vector IG or HIG was monitored by GFP expression 3 days later and the infected cells were sorted by FACSAria III Cell Sorter (BD Bioscience) for use in the RT-qPCR assay. Lentiviral vector expressing short hairpin RNA (shRNA) was produced by transfection of pCMVdeltaR8.91 (10.8 μg), pMD.G (1.2 μg) and pLKO.1-puro plasmid carrying an shRNA (12 μg) (obtained from the National RNAi Core Facility, Taipei, Taiwan) into 293T cells (28). The shRNA sequences specific for *HOXA5* and GFP were 5'-CCGCAGAAGGAGGATTGAAAT-3' and 5'-CAACAGCCACAACGTCTATAT-3', respectively. OSCC cells infected with shHOXA5-expressing lentivirus vector at an MOI of 5 were selected by incubating with 2 μg/ml puromycin (MilliporeSigma) for 2 days. Then cells were maintained in the presence of 1 μg/ml puromycin. Cells infected with shGFP-expressing lentiviral vector were used as a control.

Luciferase reporter assay. Two pGL2b plasmids (Promega Corporation) containing a wild-type and an AP-1 motif mutated p53 promoters inserted into polycloning sites upstream of the firefly luciferase (FL) reporter gene (29) were used in the assay. Each of the pGL2b plasmids were cotransfected with pRL-TK *Renilla* luciferase (RL) control reporter vector (Promega Corporation) into cells by using Lipofectamine 2000 (Thermo Fisher Scientific, Inc.). At 48 h post-transfection, cells were washed twice with phosphate buffered saline (PBS), lysed in the Luciferase assay lysis buffer (Promega Corporation), scraped from the culture dish and transferred to a tube. After vortex and centrifugation at 10,000 x g for 1 min at room temperature, the supernatant was collected for quantification of luciferase activity using Dual-Luciferase Reporter Assay System (Promega Corporation) according to the manufacturer's protocol. The relative transcriptional activity was determined as the ratio of FL to RL.

Cell viability analysis by MTS assay. Cells were seeded onto replicate 96-well plates at a density of 2,000 cells/well on day 0. The cell viability was determined on day 4 by the MTS assay using the CellTiter Aqueous One Solution Cell Proliferation Assay kit (Promega Corporation).

Cell necrosis assay. Cells were seeded onto replicate 6-well plate at a density of $6x10^4$ cells/well on day 0. On day 1, the cells were washed with PBS and cultured in the medium containing 2 μg/ml cisplatin. Three days later, the cells were harvested with trypsin, fixed with 70% ethanol for 24 h, stained with propidium iodide (MilliporeSigma) for 30 min at 37˚C and analyzed by FACSCalibur (BD Biosciences). The proportion of necrotic cells in sub-G1 area was quantified using CellQuest Pro software (BD Biosciences).

In vivo experiments. The *in vivo* experiments were conducted in accordance with the principles of laboratory animal care at the National Institutes of Health and with the approval of the Institutional Animal Care and Use Committee at National Chung Cheng University, Taiwan, R.O.C. (IACUC no. 1080401). A total of 29 female athymic BALB/c nude mice (5-6 weeks old; ~25 g) were supplied by National Laboratory Animal Center (Taipei, Taiwan). The housing conditions of the mice were as follows: 12-h light/dark cycle; temperatures of 18-23˚C with 40-60% humidity; and water and food accessible at all times. Following the induction of anesthesia using 2% isoflurane for four minutes and 1.5% maintenance, the mice were inoculated with $5x10^6$ OC2 cells in the right dorsal flank. When the tumor volumes reached ~100 mm^3 (16 days after tumor implantation), the mice received intraperitoneal injections of PBS or cisplatin at a weekly dose of 3 mg/kg for a total of six treatments. Tumor length (L) and width (W) were measured daily with calipers and tumor volumes were calculated using the formula (LxWxW/2). At the experimental endpoint (60 days after tumor implantation), all mice were humanely sacrificed under a 2% isoflurane gas anesthesia by cervical dislocation. Mortality was verified through a physical examination for the absence of cardiac activity and respiration.

Statistical analyses. Wilcoxon signed rank test was used to test the difference in fold-change of RNA expression between paired normal and tumor samples. One-way ANOVA was

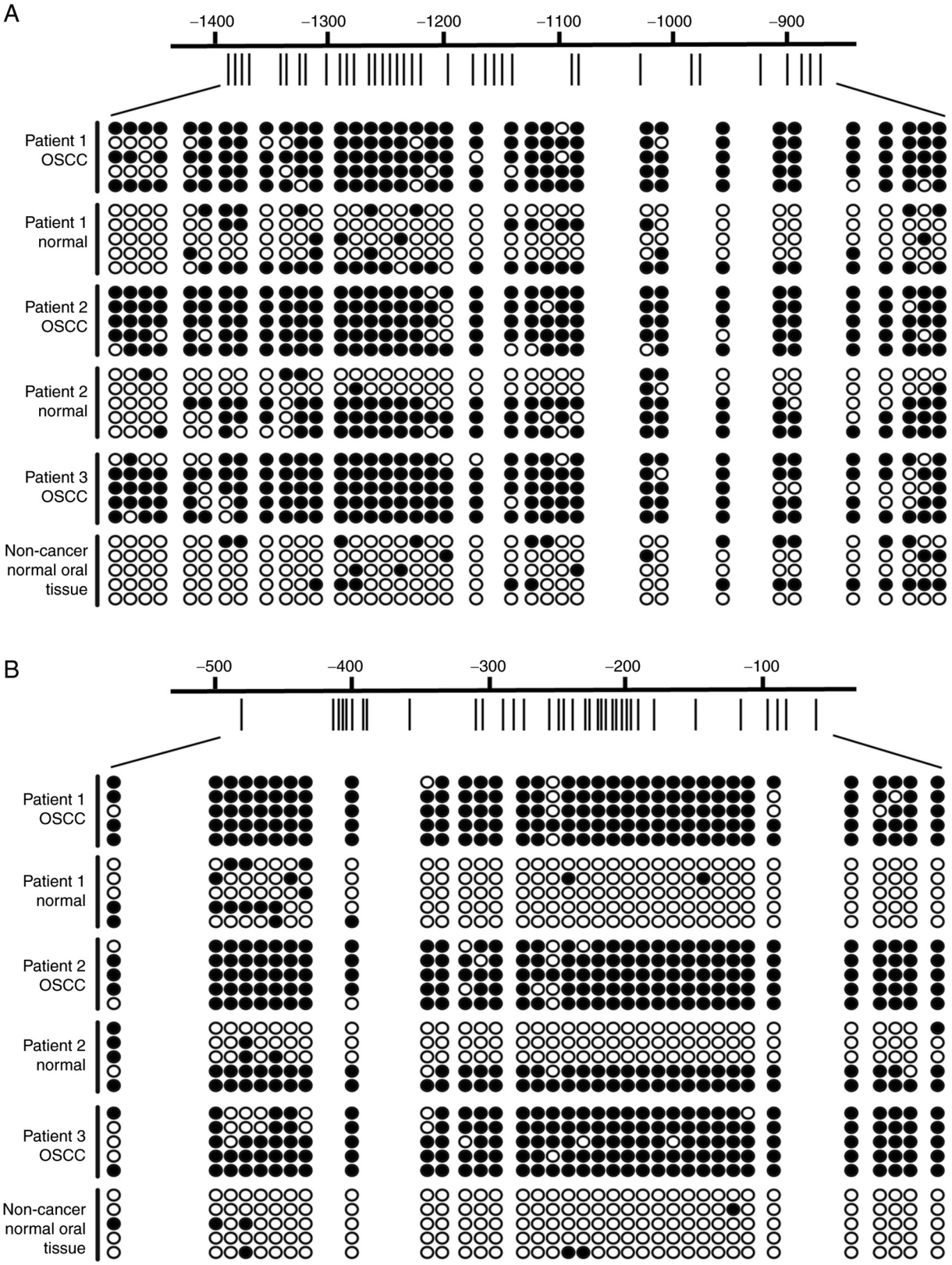


Figure 1. Bisulfite sequencing analysis of the promoter regions for *HOXA5*. The promoter regions (A) from -1423 to -841 and (B) from -505 to -31 upstream of the transcription start site of *HOXA5* comprised 72 CpG sites. The CpG sites are indicated by vertical bars. A representative bisulfite sequencing assay was applied to OSCC and normal oral tissues. For each tissue sample, five randomly chosen clones were sequenced and the methylation statuses of the 72 CpG sites are indicated by the circles: Closed and open circles represent methylated and unmethylated CpG sites, respectively.

conducted for the comparion of methylation level and relative protein expression among three dose levels of 5-Aza-dC followed by Dunnett's test for the multiple comparison against the control group. Student's t-tests were performed for the comparion of relative RNA expression, cell viability, and cell necrosis between two treatment groups. For the comparison of

Table I. Performance of 44 CpG sites of HOXA5 for detecting OSCC.

Probe	UCSC RefGene Group	Mean Δβ	Discrimination statistics		
			AUC	(95% CI)	P-value
cg00809969	3'-UTR	0.10	0.84	(0.72, 0.96)	<0.0001
cg19701577	3'-UTR	0.15	0.91	(0.83, 0.99)	<0.0001
cg14974749	Body	0.28	0.93	(0.87, 1.00)	<0.0001
cg20974609	Body	0.13	0.77	(0.62, 0.91)	0.0003
cg10592111	Body	0.09	0.75	(0.60, 0.89)	0.0011
cg16139219	Body	0.09	0.76	(0.61, 0.91)	0.0007
cg11724970	Body	0.13	0.77	(0.63, 0.91)	0.0002
cg05076221	Body	0.10	0.79	(0.65, 0.93)	<0.0001
cg23936031	1st Exon	0.10	0.69	(0.53, 0.85)	0.0178
cg09549073	5'-UTR	0.08	0.7	(0.54, 0.86)	0.0124
cg04863892	TSS200	0.07	0.66	(0.49, 0.83)	0.0615
cg09207400	TSS200	0.07	0.7	(0.54, 0.85)	0.0134
cg19759481	TSS200	0.09	0.69	(0.53, 0.86)	0.0188
cg02916332	TSS1500	0.09	0.74	(0.59, 0.89)	0.0021
cg17569124	TSS1500	0.08	0.72	(0.56, 0.88)	0.0062
cg02005600	TSS1500	0.09	0.74	(0.59, 0.90)	0.0018
cg25307665	TSS1500	0.15	0.8	(0.67, 0.93)	<0.0001
cg14014955	TSS1500	0.09	0.74	(0.58, 0.89)	0.0033
cg02646423	TSS1500	0.10	0.7	(0.54, 0.86)	0.0151
cg20517050	TSS1500	0.15	0.8	(0.66, 0.93)	<0.0001
cg23204968	TSS1500	0.12	0.75	(0.60, 0.91)	0.0013
cg14058329	TSS1500	0.20	0.9	(0.81, 0.99)	<0.0001
cg03207666	TSS1500	0.17	0.9	(0.81, 0.99)	<0.0001
cg23454797	TSS1500	0.13	0.8	(0.67, 0.93)	<0.0001
cg12015737	TSS1500	0.28	0.91	(0.82, 1.00)	<0.0001
cg08070327	TSS1500	0.17	0.87	(0.76, 0.98)	<0.0001
cg25506432	TSS1500	0.12	0.87	(0.76, 0.98)	<0.0001
cg16997642	TSS1500	0.20	0.89	(0.80, 0.99)	<0.0001
cg20817131	TSS1500	0.19	0.91	(0.81, 1.00)	<0.0001
cg14013695	TSS1500	0.22	0.91	(0.83, 1.00)	<0.0001
cg25390165	TSS1500	0.15	0.9	(0.81, 1.00)	<0.0001
cg01323381	TSS1500	0.26	0.92	(0.85, 1.00)	<0.0001
cg19643053	TSS1500	0.27	0.94	(0.87, 1.00)	<0.0001
cg05774699	TSS1500	0.20	0.91	(0.84, 0.99)	<0.0001
cg26023912	TSS1500	0.18	0.91	(0.83, 0.99)	<0.0001
cg14882265	TSS1500	0.16	0.89	(0.80, 0.99)	<0.0001
cg17432857	TSS1500	0.25	0.94	(0.87, 1.00)	<0.0001
cg00969405	TSS1500	0.25	0.93	(0.87, 1.00)	<0.0001
cg07049592	TSS1500	0.19	0.93	(0.85, 1.00)	<0.0001
cg02106682	TSS1500	0.19	0.93	(0.85, 1.00)	<0.0001
cg03368099	TSS1500	0.21	0.92	(0.82, 1.00)	<0.0001
cg01748892	TSS1500	0.16	0.88	(0.78, 0.98)	<0.0001
cg13694927	TSS1500	0.17	0.88	(0.77, 0.98)	<0.0001
cg03744763	TSS1500	0.18	0.86	(0.75, 0.98)	<0.0001

OSCC, oral squamous cell carcinoma; Δβ, β_{tumor}-β_{normal}; AUC, area under the receiver operating characteristic curve; CI, confidence interval.

tumor growth rates, generalized linear models with generalized estimated equations were used to account for the correlation between the repeated measurements. The interaction terms between time and group in the generalized linear models were used to evaluate the difference in tumor growth rates. Analyses were performed using SAS version 9.4 (SAS Institute).

Results

HOXA5 hypermethylation as a biomarker for OSCC detection. We have previously investigated the methylation levels of three CpG sites (-1324, -479 and +187 related to TSS) in the promoter region of *HOXA5* using the Illumina GoldenGate Methylation Array (Illumina, Inc). The methylation levels (presented as β values) at the three query sites (-1324, -479 and +187) were all significantly higher in the OSCC tissues than in normal oral tissues and the -1324 site was effective for detecting OSCC with an AUC of 0.83 (specificity=87%, sensitivity=80%) (13). To validate the array data, the present study analyzed the methylation status of *HOXA5* promoter regions from -1423 to -841 and from -505 to -31 in several oral tissue specimens by using bisulfite sequencing assay. The comparison of three normal tissues with low β values (β=0.06, 0.08 and 0.03 for the -1324 site) indicated much higher methylation density in the promoter region of three OSCC tissues with high β values (β=0.31, 0.32 and 0.43 for the -1324 site) (Fig. 1).

To obtain more-complete information on the methylation status of *HOXA5*, the present study applied the Infinium MethylationEPIC BeadChip assay (Illumina, Inc.) to 25 paired OSCC and adjacent normal tissue specimens. Among the 44 CpG sites of *HOXA5* analyzed using the BeadChip assay, 43 presented significantly higher methylation in OSCC tissues than in the normal oral tissues, with 25 CpG sites exhibiting AUCs of >0.80 (Table I). Comparison of *HOXA5* RNA expression between these paired normal oral and OSCC tissue specimens yielded results consistent with those obtained by the BeadChip assay. The median *HOXA5* expression level was 2.06-fold higher in normal tissues than in OSCC tissues (interquartile range=2.89; P<0.005; Fig. 2). These results indicated that *HOXA5* is hypermethylated in OSCC tissues and that *HOXA5* hypermethylation might hold great potential as a biomarker for detecting OSCC.

HOXA5 expression regulated by DNA methylation. The present study treated the OSCC cell lines OCSL and OC2 using the demethylating agent 5-Aza-dC to determine the correlation between *HOXA5* methylation status and its gene expression and to observe whether *HOXA5* expression could be augmented. Quantitative MSP analysis revealed that *HOXA5* methylation levels decreased in a dose-dependent manner after treatment using 5-Aza-dC (Fig. 3A). *HOXA5* expression was observed to increase in the protein in both cell lines, which was consistent with the reduced DNA methylation (Fig. 3B). Increased p53 expression was also observed in OC2 after 5-Aza-dC treatment, however, p53 expression was negligible in OCSL before and after 5-Aza-dC treatment (Fig. 3B). The results suggested that the methylation level and gene expression of *HOXA5* were negatively correlated and that DNA methylation plays an important role in *HOXA5* downregulation in OSCC.

HOXA5 upregulates p53 transcriptional activity in OSCC. A previous study found that HOXA5 is a p53 transcription factor and induces the apoptosis of breast cancer cells (16). To determine if HOXA5 plays a role in regulating p53 expression and inducing OSCC cell death, the present study either overexpressed or knocked down *HOXA5* in

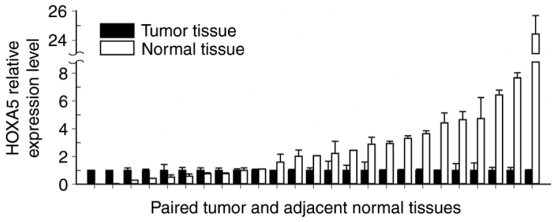


Figure 2. *HOXA5* expression levels in paired OSCC and adjacent normal tissues. *HOXA5* mRNA levels were compared between the paired normal oral tissue and OSCC tissue specimens, with latter assigned a value of 1. Error bars indicate standard deviations. OSCC, oral squamous cell carcinoma.

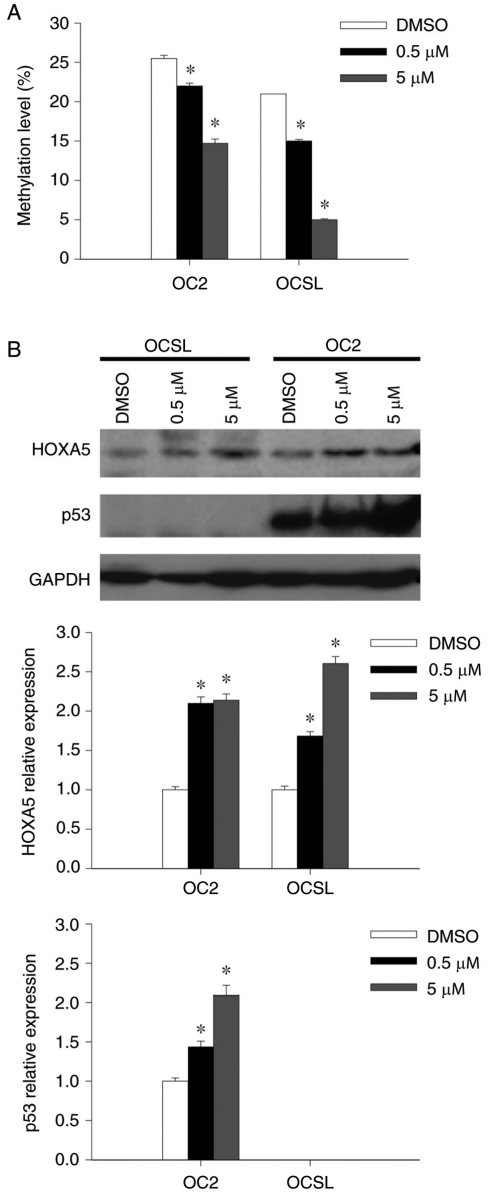


Figure 3. *HOXA5* methylation and expression levels following 5-Aza-dC treatment. (A) OC2 and OCSL cells were treated with DMSO, 0.5 μM 5-Aza-dC, or 5 μM 5-Aza-dC for 3 days. The methylation level of *HOXA5* was measured using quantitative methylation-specific PCR. (B) The cells were lysed followed by extraction of proteins 3 days after DMSO or 5-Aza-dC treatment and the protein levels of HOXA5, p53 and GAPDH were determined using western blotting (top panel). HOXA5 and p53 proteins were quantified using ImageJ software and normalized relative to GAPDH (middle and bottom panels). Protein levels of cells treated with DMSO were assigned a value of 1. Error bars indicate standard deviations. *P<0.05. 5-Aza-dC, 5-aza-2'-deoxycytidine; OSCC, oral squamous cell carcinoma.

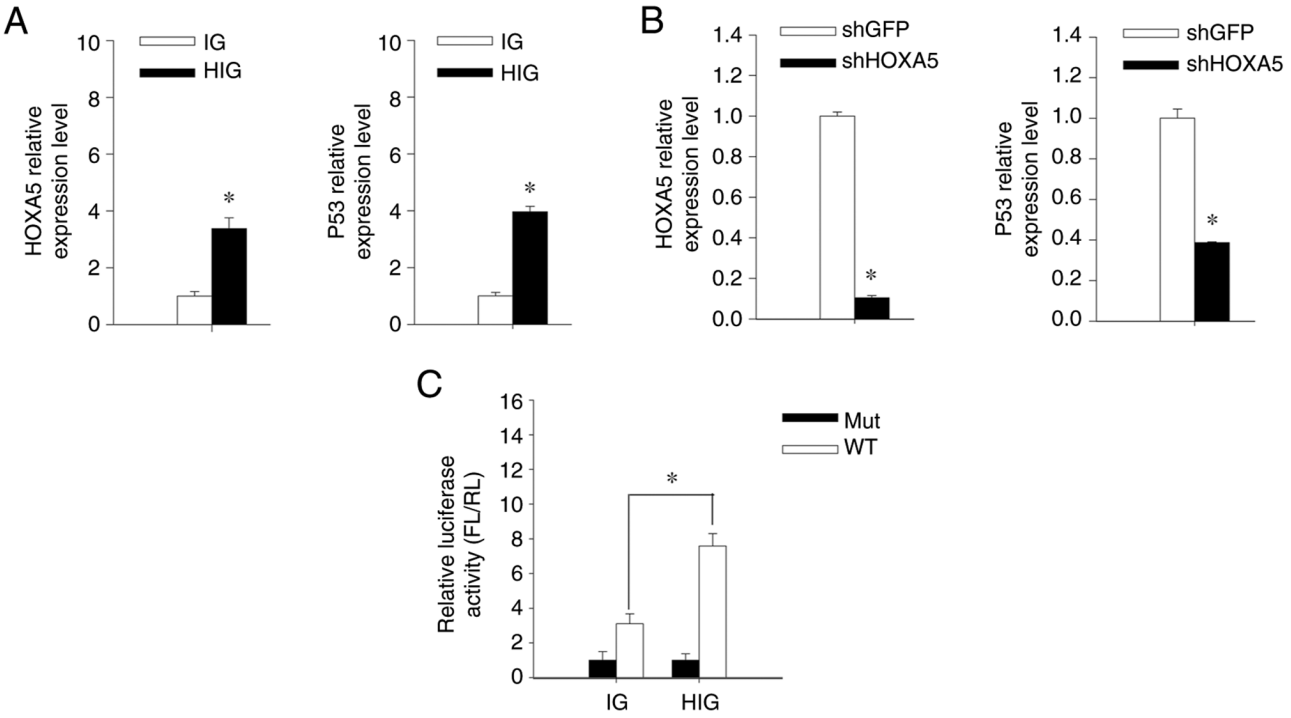


Figure 4. HOXA5 upregulates p53 expression in OSCC. (A) OC2 cells were transduced using IG or HIG followed by fluorescence-activated cell sorting and the mRNA levels of HOXA5 and p53 in OC2 were quantified using RT-qPCR. The expression level of each IG-transduced cell was assigned a value of 1. (B) OC2 cells were transduced using lentiviral vector carrying shHOXA5 or shGFP and selected using puromycin. The mRNA expression of HOXA5 and p53 in OC2 were quantified using RT-qPCR. The expression level of each shGFP-transduced cell was assigned a value of 1. (C) The IG- and HIG-transduced OC2 cells were transfected with pGL2b-WTp53-FL or pGL2b-Mutp53-FL and cotransfected with pRL-TK to act as internal control reporters. Bioluminescence intensities of FL and RL were measured using a luminometer and the luciferase activity was calculated from the FL-to-RL ratio. The IG-transduced OC2 cells transfected with pGL2b-Mutp53-FL were assigned a value of 1. Error bars indicate standard deviations. *P<0.05. WT, pGL2b-WTp53-FL; Mut, pGL2b-Mutp53-FL. OSCC, oral squamous cell carcinoma; IG, control lentiviral vector; HIG, HOXA5-expressing lentiviral vector; RT-qPCR, reverse transcription-quantitative PCR; sh, short hairpin; FL, firefly luciferase; RL, *Renilla* luciferase; Mut, mutant; WT, wild-type.

the OC2 cell line by employing lentiviral vector-mediated *HOXA5* transfer or RNA interference. When *HOXA5* was overexpressed, the expression of p53 was also upregulated in OC2 (Fig. 4A). By contrast, *HOXA5* knockdown using the lentiviral-vector-delivered shRNA targeting *HOXA5* downregulates the p53 expression (Fig. 4B). These results indicated a positive correlation between the expression levels of HOXA5 and p53. To further determine if p53 expression was transcriptionally regulated by HOXA5, we transfected OC2 cells using the wild-type (pGL2b-WTp53-FL) or mutant-type (pGL2b-Mutp53-FL) p53-responsive luciferase expression plasmid followed by performing a luciferase reporter assay. A greater transcriptional activity of luciferase in *HOXA5*-overexpressed cells was observed compared with control cells (Fig. 4C). These results indicated that HOXA5 may act as a transcription factor in the upregulation of p53 expression in OC2 cells.

Restoration of HOXA5 reduces OSCC cell viability. Previous studies have demonstrated that p53 affects the viability of various cancer cell types via mechanisms such as apoptosis, cell-cycle arrest and senescence (30,31); the present study also demonstrated that HOXA5 can upregulate p53 expression in OC2 cells. An MTS assay was performed to measure the viability of *HOXA5*-overexpressed OC2 cells and determine if HOXA5-upregulated p53 expression influences the viability of OSCC cells. The results in Fig. 5A revealed that the viability of *HOXA5*-overexpressed cells was inhibited relative to the IGs. Cisplatin is a common chemotherapy drug for treating various cancers, including OSCC (32). Nevertheless, the therapeutic effect of cisplatin can be attenuated by the loss of p53 function in cancer cells, which also induces resistance to cisplatin (33). *HOXA5*-overexpressed cells were exposed to cisplatin and then cell viability was analyzed using the MTS assay to determine whether HOXA5-upregulated p53 expression enhanced the sensitivity of cisplatin. The results in Fig. 5A revealed that the viability of *HOXA5*-overexpressed cells was inhibited relative to the IGs after exposure to cisplatin. Furthermore, a cell necrosis assay confirmed that *HOXA5* overexpression induces necrosis in OSCC cells and hence reduces their viability (Fig. 5B).

HOXA5 enhances the therapeutic effect of cisplatin in OSCC in vivo. The *in vitro* experiments indicated that *HOXA5* can reduce cell viability and enhance the therapeutic effect of cisplatin in OC2 cells. Cisplatin was administered to mice bearing subcutaneous OC2 xenografts to confirm the role of *HOXA5* in enhancing the efficiency of chemotherapy against OSCC *in vivo*. In comparison with the IG/PBS group, cisplatin treatment slightly suppressed tumor growth in the IG/cisplatin group. *HOXA5* overexpression further enhanced the therapeutic effect of cisplatin in the HIG/cisplatin group, indicating a strong antitumor effect from combining *HOXA5* and cisplatin (Fig. 6).

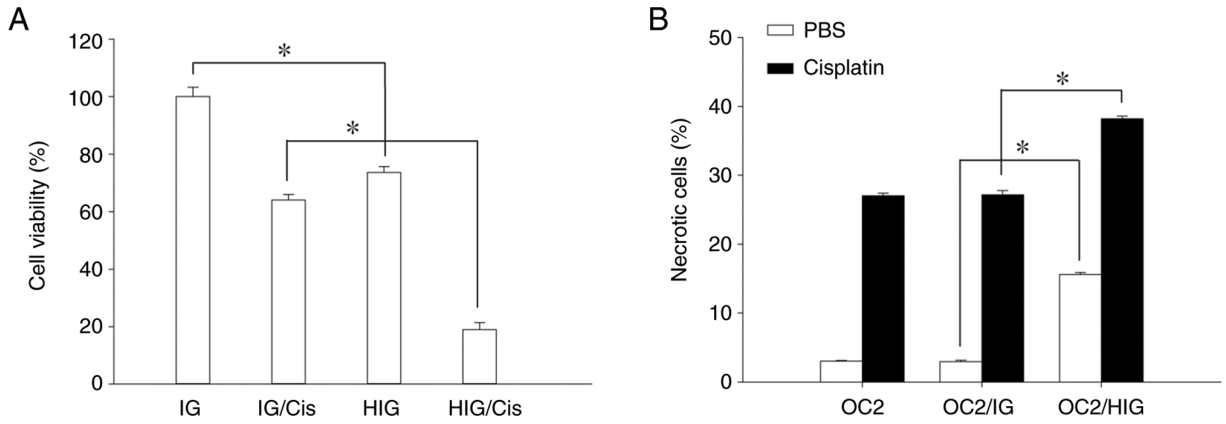


Figure 5. Effect of *HOXA5* restoration on OSCC cell viability. (A) The IG- and HIG-transduced OC2 cells were seeded onto culture plates on day 0 and the cells were treated with 2 μg/ml cisplatin on day 1. Cell viability was analyzed on day 4 using MTS assay. (B) The IG- and HIG-transduced OC2 cells were treated with 2 μg/ml cisplatin or PBS for 3 days and stained with propidium iodide and then analyzed using flow cytometry. The proportions of necrotic cells are presented. Error bars indicate standard deviations. *P<0.05. OSCC, oral squamous cell carcinoma; IG, control lentiviral vector; HIG, HOXA5-expressing lentiviral vector; IG/Cis, IG/cisplatin; HIG/Cis, HIG/cisplatin.

Discussion

The high-throughput methylation array applied in the present study revealed that *HOXA5* was hypermethylated in OSCC tissues, an observation that was also confirmed by the bisulfite sequencing analysis (Fig. 1). Hypermethylation of *HOXA5* has been identified as a mechanism that suppresses its expression in breast and skin tumorigenesis (16,34). Consistent with RT-qPCR data that revealed the *HOXA5* expression level to be lower in OSCC tissues than in normal oral tissues (Fig. 2), *HOXA5* expression can be promoted in OSCC cells after treating the cells using the demethylating agent 5-Aza-dC (Fig. 3).

While it is clear that DNA methylation plays an important role in inhibiting *HOXA5* expression in OSCC, other epigenetic regulations including histone hypoacetylation were also considered as contributing events in the process of oral carcinogenesis (11). *HOXA5* expression in OSCC cells increased following 5-Aza-dC treatment, while no such effects occurred following treatment with histone deacetylase inhibitor trichostatin A (TSA) (data not shown). Consistent with the previous study (35) finding that DNA methylation was more dominant than histone hypoacetylation in regulating *HOXA5* expression in breast cancer cells, in which TSA treatment did not reactivate the silenced *HOXA5*, *HOXA5* hypermethylation is the main mechanism underlying the inhibition of *HOXA5* expression in OSCC cells.

The present study demonstrated that restoring *HOXA5* expression not only inhibited OSCC growth *in vitro* but also enhanced the therapeutic effect of cisplatin both *in vitro* and *in vivo*. These effects were in part achieved by *HOXA5* upregulating p53 expression, which has also been demonstrated to activate an apoptotic pathway in breast cancer cells (16). p53 upregulation has also been demonstrated to subsequently increase the expression of its downstream target genes, *p21* and *Bax*, in OSCC cells treated with natural compounds and aspirin (36-38). However, p53 mutations have been reported to occur in ~50% of human cancers (39) and it is also the gene that most frequently mutates in OSCC and causes failure of cisplatin treatments and poor disease outcomes (40). A previous

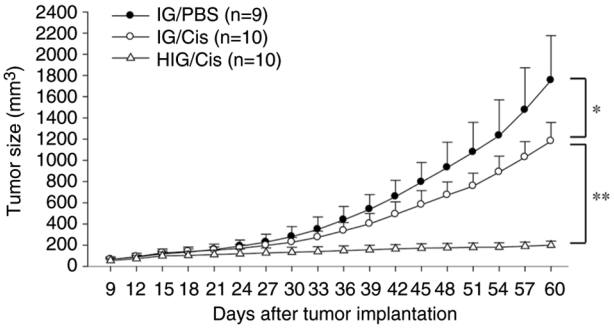


Figure 6. *HOXA5* enhances the therapeutic effect of cisplatin in the animal tumor model. The IG- and HIG-transduced OC2 cells were subcutaneously implanted into the dorsal flanks of nude mice. When the tumor volumes reached ~100 mm^3 (at 16 days after tumor implantation), the mice received six weekly intraperitoneal injections of PBS or cisplatin at a dose of 3 mg/kg. Error bars indicate standard deviations. *P<0.05. **P<0.001. IG, control lentiviral vector; HIG, HOXA5-expressing lentiviral vector; IG/Cis, IG/cisplatin; HIG/Cis, HIG/cisplatin.

study on the p53-mutated breast cancer cell line Hs578T found that *HOXA5* could alternatively induce cell apoptosis via a p53-independent pathway through the activation of caspase-2 and caspase-8 (41). *HOXA5* restoration therefore might still be able to activate caspases in the case of p53-mutated OSCC, causing p53-independent apoptosis.

Through monitoring the growth curves of tumors, it was found that *HOXA5* greatly enhanced the therapeutic effect of cisplatin *in vivo*, achieving a major reduction in tumor size. However, at the experimental endpoint, all mice were humanely sacrificed without surgical excision of tumors. As a result, the present study was unable to show the appearance and the actual size of excised tumors.

In summary, the present study found a differential pattern of *HOXA5* methylation between normal oral and OSCC tissues, indicating that *HOXA5* hypermethylation is a reliable biomarker for detecting OSCC. The data suggested that *HOXA5* is a downregulated proapoptotic gene in OSCC and that restoring expression can help to treat OSCC regardless of the presence of chemotherapy.

Acknowledgements

Not applicable.

Funding

The present study was supported in part by the Ministry of Science and Technology of Taiwan (grant no. MOST105-2320-B-194-003) and Ditmanson Medical Foundation Chia-Yi Christian Hospital (grant no. R108-018).

Availability of data and materials

The data generated in the present study may be requested from the corresponding author.

Authors' contributions

YC and SL performed the laboratory experiments and drafted the manuscript. YeL contributed to the laboratory work. YuL performed analysis and interpretation of data. YiL and CT conceived and coordinated the overall study and revised the manuscript. YiL and CT confirm the authenticity of all the raw data. All authors read and approved the final manuscript.

Ethics approval and consent to participate

Tissue samples were collected from patients after obtaining written informed consent in accordance with a protocol approved by the Institutional Review Board of China Medical University Hospital, Taiwan, R.O.C. (IRB no. CMUH102-REC1-054). All animal experiments were conducted in accordance with the principles of laboratory animal care at the National Institutes of Health and with the approval of the Institutional Animal Care and Use Committee at National Chung Cheng University, Taiwan, R.O.C. (IACUC no. 1080401).

Patient consent for publication

Not applicable.

Competing interests

The authors declare that they have no competing interests.

References

1. Torre LA, Bray F, Siegel RL, Ferlay J, Lortet-Tieulent J and Jemal A: Global cancer statistics, 2012. CA Cancer J Clin 65: 87-108, 2015.
2. Ferlay J, Soerjomataram I, Dikshit R, Eser S, Mathers C, Rebelo M, Parkin DM, Forman D and Bray F: Cancer incidence and mortality worldwide: Sources, methods and major patterns in GLOBOCAN 2012. Int J Cancer 136: E359-e386, 2015.
3. Ministry of Health and Welfare: 2021 Cancer Registry Annual Report. https://twcr.tw/wp-content/uploads/2024/02/Top-10-cancers-in-Taiwan-2021.pdf. Accessed December 18, 2024.
4. Health Promotion Administration, Ministry of Health and Welfare: 2023 Health Promotion Administration Annual Report. https://www.hpa.gov.tw/EngPages/Detail.aspx?nodeid=1070&pid=18165. Accessed December 18, 2024.
5. Warnakulasuriya S: Global epidemiology of oral and oropharyngeal cancer. Oral Oncol 45: 309-316, 2009.
6. Pedruzzi PAG, Kowalski LP, Nishimoto IN, Oliveira BV, Tironi F and Ramos GHA: Analysis of prognostic factors in patients with oropharyngeal squamous cell carcinoma treated with radiotherapy alone or in combination with systemic chemotherapy. Arch Otolaryngol Head Neck Surg 134: 1196-1204, 2008.
7. Ishida K, Tomita H, Nakashima T, Hirata A, Tanaka T, Shibata T and Hara A: Current mouse models of oral squamous cell carcinoma: Genetic and chemically induced models. Oral Oncol 73: 16-20, 2017.
8. Lin CS, Lin YC, Adebayo BO, Wu A, Chen JH, Peng YJ, Cheng MF, Lee WH, Hsiao M, Chao TY and Yeh CT: Silencing JARID1B suppresses oncogenicity, stemness and increases radiation sensitivity in human oral carcinoma. Cancer Lett 368: 36-45, 2015.
9. Koch FP, Kunkel M, Biesterfeld S and Wagner W: Diagnostic efficiency of differentiating small cancerous and precancerous lesions using mucosal brush smears of the oral cavity-a prospective and blinded study. Clin Oral Investig 15: 763-769, 2011.
10. Hadzic S, Gojkov-Vukelic M, Pasic E and Dervisevic A: Importance of early detection of potentially malignant lesions in the prevention of oral cancer. Mater Sociomed 29: 129-133, 2017.
11. D'Souza W and Saranath D: Clinical implications of epigenetic regulation in oral cancer. Oral Oncol 51: 1061-1068, 2015.
12. Hema KN, Smitha T, Sheethal HS and Mirnalini SA: Epigenetics in oral squamous cell carcinoma. J Oral Maxillofac Pathol 21: 252-259, 2017.
13. Li YF, Hsiao YH, Lai YH, Chen YC, Chen YJ, Chou JL, Chan MW, Lin YH, Tsou YA, Tsai MH and Tai CK: DNA methylation profiles and biomarkers of oral squamous cell carcinoma. Epigenetics 10: 229-236, 2015.
14. Lizen B, Moens C, Mouheiche J, Sacré T, Ahn MT, Jeannotte L, Salti Aand Gofflot F: Conditional loss of Hoxa5 function early after birth impacts on expression of genes with synaptic function. Front Mol Neurosci 10: 369, 2017.
15. Landry-Truchon K, Houde N, Boucherat O, Joncas FH, Dasen JS, Philippidou P, Mansfield JH and Jeannotte L: HOXA5 plays tissue-specific roles in the developing respiratory system. Development 144: 3547-3561, 2017.
16. Raman V, Martensen SA, Reisman D, Evron E, Odenwald WF, Jaffee E, Marks J and Sukumar S: Compromised HOXA5 function can limit p53 expression in human breast tumours. Nature 405: 974-978, 2000.
17. Kikuyama M, Takeshima H, Kinoshita T, Okochi-Takada E, Wakabayashi M, Akashi-Tanaka S, Ogawa T, Seto Y and Ushijima T: Development of a novel approach, the epigenome-based outlier approach, to identify tumor-suppressor genes silenced by aberrant DNA methylation. Cancer Lett 322: 204-212, 2012.
18. Conway K, Edmiston SN, May R, Kuan PF, Chu H, Bryant C, Tse CK, Swift-Scanlan T, Geradts J, Troester MA and Millikan RC: DNA methylation profiling in the Carolina breast cancer study defines cancer subclasses differing in clinicopathologic characteristics and survival. Breast Cancer Res 16: 450, 2014.
19. Daugaard I, Dominguez D, Kjeldsen TE, Kristensen LS, Hager H, Wojdacz TK and Hansen LL: Identification and validation of candidate epigenetic biomarkers in lung adenocarcinoma. Sci Rep 6: 35807, 2016.
20. Martinez R, Carmona FJ, Vizoso M, Rohde V, Kirsch M, Schackert G, Ropero S, Paulus W, Barrantes A, Gomez A and Esteller M: DNA methylation alterations in grade II- and anaplastic pleomorphic xanthoastrocytoma. BMC Cancer 14: 213, 2014.
21. Kanai M, Hamada J, Takada M, Asano T, Murakawa K, Takahashi Y, Murai T, Tada M, Miyamoto M, Kondo S and Moriuchi T: Aberrant expressions of HOX genes in colorectal and hepatocellular carcinomas. Oncol Rep 23: 843-851, 2010.
22. Rodini CO, Xavier FCA, Paiva KBS, De Souza Setúbal Destro MF, Moyses RA, Michaluarte P, Carvalho MB, Fukuyama EE; Head And Neck Genome Project Gencapo; Tajara EH, *et al*: Homeobox gene expression profile indicates HOXA5 as a candidate prognostic marker in oral squamous cell carcinoma. Int J Oncol 40: 1180-1188, 2012.
23. Livak KJ and Schmittgen TD: Analysis of relative gene expression data using real-time quantitative PCR and the 2(-Delta Delta C(T)) method. Methods 25: 402-408, 2001.
24. Wong DY, Chang KW, Chen CF and Chang RC: Characterization of two new cell lines derived from oral cavity human squamous cell carcinomas-OC1 and OC2. J Oral Maxillofac Surg 48: 385-390, 1990.

25. Lai YH, He RY, Chou JL, Chan MWY, Li YF and Tai CK: Promoter hypermethylation and silencing of tissue factor pathway inhibitor-2 in oral squamous cell carcinoma. J Transl Med 12: 237, 2014.
26. Gillan L, Matei D, Fishman DA, Gerbin CS, Karlan BY and Chang DD: Periostin secreted by epithelial ovarian carcinoma is a ligand for alpha(V)beta(3) and alpha(V)beta(5) integrins and promotes cell motility. Cancer Res 62: 5358-5364, 2002.
27. Shichinohe T, Bochner BH, Mizutani K, Nishida M, Hegerich-Gilliam S, Naldini L and Kasahara N: Development of lentiviral vectors for antiangiogenic gene delivery. Cancer Gene Ther 8: 879-889, 2001.
28. Chen YJ, Chen SY, Lovel R, Ku YC, Lai YH, Hung CL, Li YF, Lu YC and Tai CK: Enhancing chemosensitivity in oral squamous cell carcinoma by lentivirus vector-mediated RNA interference targeting EGFR and MRP2. Oncol Lett 12: 2107-2114, 2016.
29. Kirch HC, Flaswinkel S, Rumpf H, Brockmann D and Esche H: Expression of human p53 requires synergistic activation of transcription from the p53 promoter by AP-1, NF-kappaB and Myc/Max. Oncogene 18: 2728-2738, 1999.
30. Kaiser AM and Attardi LD: Deconstructing networks of p53-mediated tumor suppression in vivo. Cell Death Differ 25: 93-103, 2018.
31. Mello SS and Attardi LD: Deciphering p53 signaling in tumor suppression. Curr Opin Cell Biol 51: 65-72, 2018.
32. Andreadis C, Vahtsevanos K, Sidiras T, Thomaidis I, Antoniadis K and Mouratidou D: 5-Fluorouracil and cisplatin in the treatment of advanced oral cancer. Oral Oncol 39: 380-385, 2003.
33. Jo DW, Kim YK and Yun PY: The influence of p53 mutation status on the anti-cancer effect of cisplatin in oral squamous cell carcinoma cell lines. J Korean Assoc Oral Maxillofac Surg 42: 337-344, 2016.
34. Watson RE, Curtin GM, Hellmann GM, Doolittle DJ and Goodman JI: Increased DNA methylation in the HoxA5 promoter region correlates with decreased expression of the gene during tumor promotion. Mol Carcinog 41: 54-66, 2004.
35. Novak P, Jensen T, Oshiro MM, Wozniak RJ, Nouzova M, Watts GS, Klimecki WT, Kim C and Futscher BW: Epigenetic inactivation of the HOXA gene cluster in breast cancer. Cancer Res 66: 10664-10670, 2006.
36. Yang SH, Liao PH, Pan YF, Chen SL, Chou SS and Chou MY: The novel p53-dependent metastatic and apoptotic pathway induced by vitexin in human oral cancer OC2 cells. Phytother Res 27: 1154-1161, 2013.
37. Yeh YT, Yeh H, Su SH, Lin JS, Lee KJ, Shyu HW, Chen ZF, Huang SY and Su SJ: Phenethyl isothiocyanate induces DNA damage-associated G2/M arrest and subsequent apoptosis in oral cancer cells with varying p53 mutations. Free Radic Biol Med 74: 1-13, 2014.
38. Ho CC, Yang XW, Lee TL, Liao PH, Yang SH, Tsai CH and Chou MY: Activation of p53 signalling in acetylsalicylic acid-induced apoptosis in OC2 human oral cancer cells. Eur J Clin Invest 33: 875-882, 2003.
39. Olivier M, Hollstein M and Hainaut P: TP53 mutations in human cancers: Origins, consequences, and clinical use. Cold Spring Harb Perspect Biol 2: a001008, 2010.
40. Lindemann A, Takahashi H, Patel AA, Osman AA and Myers JN: Targeting the DNA damage response in OSCC with TP53 mutations. J Dent Res 97: 635-644, 2018.
41. Chen H, Chung S and Sukumar S: HOXA5-induced apoptosis in breast cancer cells is mediated by caspases 2 and 8. Mol Cell Biol 24: 924-935, 2004.

Copyright © 2024 Chen et al. This work is licensed under a Creative Commons Attribution-NonCommercial-NoDerivatives 4.0 International (CC BY-NC-ND 4.0) License.